

# Design of a Wideband Unidirectional Slot Antenna with Stepped Reflector for Front to Back Ratio Enhancement

Liang Lu<sup>\*</sup>, Yong-Chang Jiao, Zi-Bin Weng, and Lei Zhou

**Abstract**—A compact unidirectional slot antenna with front to back ratio (FBR) enhancement is proposed. The antenna consists of a novel compact slot driven antenna, a stepped reflector and a vertical balun from a microstrip to a parallel strip line. Better FBRs are obtained by optimizing the stepped reflector. Impedance bandwidths are enhanced by applying the balun and a pair of microstrip stub etched on the opposite side of the slot. Then, the antenna is manufactured and measured. Measured results show that the proposed antenna has a bandwidth of 76% (1.53–3.41 GHz) for  $VSWR \leq 1.5$ . In addition, from 1.7 to 3.2 GHz, the antenna gains are higher than 8.6 dBi, and the FBRs are greater than 22 dB. Good agreement between the simulated and measured results is obtained. All above indicates that the proposed antenna can be widely used in wireless communications.

## 1. INTRODUCTION

In recent years, with the rapid development of the wireless communication systems, the antennas with enhanced impedance bandwidths, good radiation performances such as high gains, stable radiation patterns, and high front to back ratios (FBRs) are getting more and more popular.

Slot antennas with attractive features such as low cost, low profile, and easy match have been widely used in the wireless communication systems. Several techniques have been proposed to improve the performance of slot antennas [1, 2]. In [1], a fork-like tuning stub or a simple rotated slot was used to enhance the operation bandwidth. By introducing a via-hole and optimizing the location of the via-hole, bandwidth of the cavity-backed slot is enhanced [2]. In the modern wireless communication systems, unidirectional antennas have been found more popular for both indoor and outdoor applications. A slot antenna with unidirectional radiation performance can be achieved by placing a reflector behind the slot antenna. Thus, the reflector can also lower the backward radiations and improve the forward gains [3–10]. Rectangle-shaped slot antenna with a ground reflector as a fundamental structure provides unidirectional radiation patterns and wide impedance bandwidths [3]. With several uniform width notched slits etched on the ground plane, the open slot antenna with high FBRs was proposed [4]. In [5], by adding special wave guiding and reflecting structures, the antenna achieved unidirectional radiations, and the max gain of the antenna increased from 3.8 dBi to 6.8 dBi. Chaimool et al. analyzed different kinds of reflectors and suggested that the  $\Lambda$ - and inverted- $\Lambda$  shaped reflectors with a horizontal plate could enhance both radiation patterns and impedance bandwidths [6]. In [7], a bow-tie antenna with  $\Gamma$ -shaped strip feed and tuning stubs earned a wide impedance matching of about 58.6% (1.58–2.89 GHz) for  $VSWR \leq 1.5$ . By the rectangle ground plane as reflector, the antenna obtained better FBRs about 17 dB across the band. In [8], by loading an appropriate circular aperture on the square metal reflector, the back radiations of the antenna were effectively reduced, and FBRs were greatly improved. Wang et al. proposed a dual-element folded dipole with FBRs higher than 20 dB [9]. With

---

*Received 18 July 2016, Accepted 26 August 2016, Scheduled 4 September 2016*

<sup>\*</sup> Corresponding author: Liang Lu (lianglu@stu.xidian.edu.cn).

The authors are with the National Key Laboratory of Antennas and Microwave Technology, Collaborative Innovation Center of Information Sensing and Understanding, Xidian University, Xi'an, Shaanxi 710071, P. R. China.

adjustable back-reflector, the dual-element slot loop antenna can get an impedance bandwidth of 77% for  $VSWR \leq 2$  and realized gains up to 10 dBi [10]. However, when the distance is fixed, the antenna can only work at a narrow band, and the radiation patterns at other bands are not ideal. In [11], a slot antenna with two pairs of back-reflectors of different distances was presented, and the antenna had FBRs greater than 17 dB. However, for high frequency, 3 GHz, the main beam of the radiation pattern in  $z$ - $y$  plane split. In addition, the separated reflectors were difficult to assemble. When the antenna was installed close to wall, the radiation characteristics, including antenna impedance matches and radiation patterns, were degraded due to the reflection from the gap between the two middle back-reflectors.

In this paper, a compact unidirectional slot antenna with continuous stepped reflector is proposed. The slot antenna works as a magnetic dipole, which is excited by a vertical balun. The balun is a transition from microstrip line to parallel strip line, and also connects the reflector and the slot driven antenna. With the balun and reflector, the radiation patterns in  $z$ - $y$  plane are improved. Better FBRs and higher gains can be obtained. A pair of microstrip stubs etched on the opposite side of the slot is proposed. The stubs can balance the reactance of the slot antenna. Thus, wide impedance bandwidths with better FBRs and higher gains are proposed. This paper is organized as follows. Section 2 describes configuration and operation mechanism for the proposed antenna. Some important parameter studies are also shown in Section 2. The simulated and measured results are summarized and discussed in Section 3. Conclusion is given in Section 4.

## 2. ANTENNA GEOMETRY AND DESIGN

Figure 1 shows the detailed geometry of the proposed antenna. Basically, the prototype of the proposed antenna consists of a slot driven antenna, a stepped reflector, a vertical balun from unbalanced microstrip line to balanced strip line and a SMA connector.

The slot driven antenna contains a polygonal slot. It is fabricated on an FR-4 substrate ( $\epsilon_r = 4.4$ ,

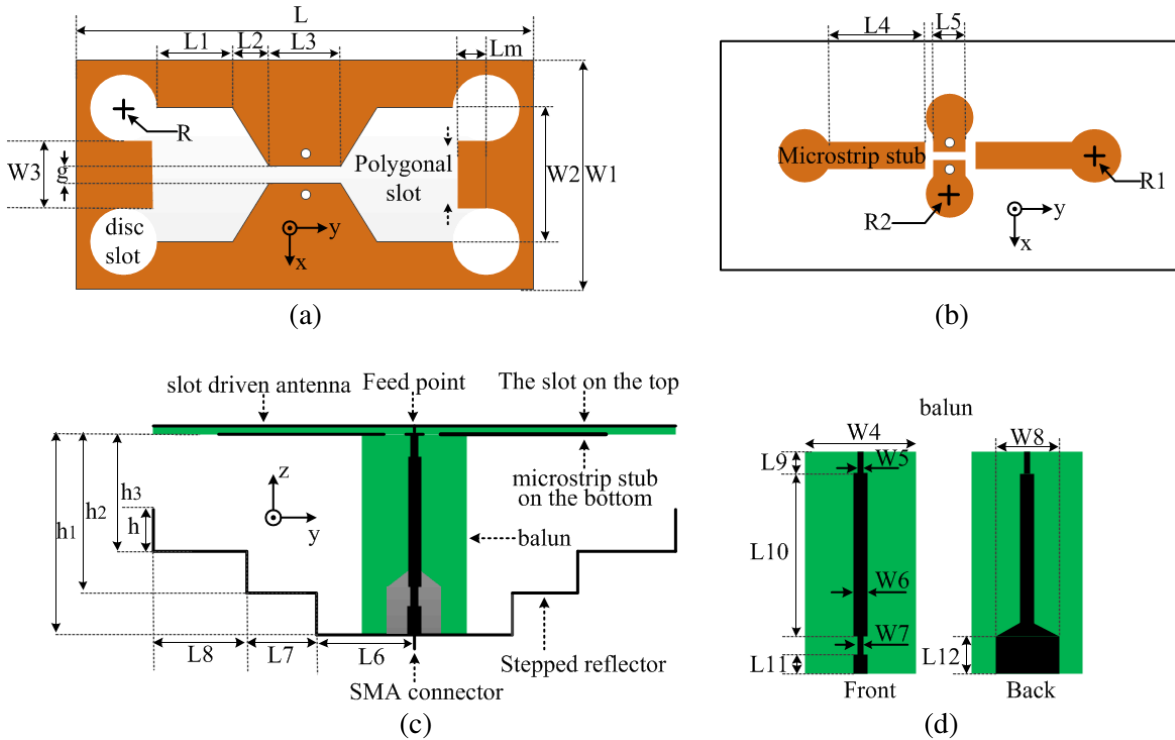


**Figure 1.** Geometry of the proposed antenna. (a) Top view of the slot driven antenna, (b) bottom view of the slot driven antenna, (c) side view and (d) front and back views of the balun.

$\tan \delta = 0.02$ ), which has a size of  $120 \text{ mm} \times 50 \text{ mm} \times 1 \text{ mm}$ . The polygonal slot consists of a narrow slot near the feed point, two wide slots and four disc slots at the corner of the wide slots. With the four disc slots, the inner perimeter of the polygonal slot, which is twice of the wavelength corresponding to the lowest frequency, becomes longer without increasing the length of the slot. Thus, the lowest resonance frequency shifts to the lower frequency bands. In our design, the calculated lowest resonance frequency is set at 1.5 GHz with a corresponding wavelength of 200 mm. The relations between the parameters and the calculated lowest resonance frequency ( $f_L$ ) are list as follows:

$$f_L = \frac{300}{\lambda_L} \tag{1}$$

$$\lambda_L = 2 \times \left( L_3/2 + \sqrt{(L_2)^2 + (W_2/2 - g/2)^2} + L_1 + 1.5 \times \pi \times R + W_3/2 + L_m \right) \tag{2}$$

where  $\lambda_L$  (in mm) is corresponding wavelength of the calculated lowest resonance frequency.

On the bottom of the substrate, a pair of microstrip stubs (the black part in Fig. 1(a)) is etched 7.5 mm apart from the feed point (the white point in Fig. 1(a)) to improve the impedance matching. Fig. 2 shows the input impedance of the antennas with and without the microstrip stubs. As shown in the figure, both the input resistance and reactance become smooth over the whole frequencies when the pair of microstrip stubs is used, and this makes it easy to adjust the real part of the input impedance around  $50 \Omega$  and the imaginary part around  $0 \Omega$ .

The slot driven antenna is excited by a balun etched on the FR-4 dielectric with a thickness of 1 mm. The balun is a transition from a microstrip line to a parallel strip line. The end of the parallel strip line connects to the feed point while the end of the microstrip line connects to a SMA connector, as shown in Fig. 1(b). Thus, the balun is also a mechanical support connecting the reflector and the slot driven antenna. Moreover, the common mode current on the reflector from the driven antenna is reduced due to the connecting of the balun. Therefore, the radiation patterns in  $z$ - $y$  plane are improved.

In order to obtain a good unidirectional radiation characteristic over the operating band, a stepped reflector is designed. The reflector is made of 0.8 mm thick aluminum and has a symmetrical structure, as shown in Figs. 1(a) and 1(b). The distances between the stepped reflector and the driven slot antenna are  $h_1$ ,  $h_2$  and  $h_3$ .

Figure 3(a) shows the performance of gains and FBRs with stepped reflector and single-plate plane reflector. The single-plate plane reflector has different distances  $h$ , selected as  $h_1$ ,  $h_2$  and  $h_3$ , respectively. As shown in the figure, the antenna can only generate a narrow band with the single-plate reflector, and the performance of the gains and FBRs are not good. The reason is explained as follows.  $h$  is selected as the quarter wavelength of resonance frequency to get in-phase wave. When the frequency increases or decreases,  $h$  is not quarter wavelength, and the in-phase wave cannot be produced within broad band. On the other hand, the out-phase wave may produce, which makes the gains and FBRs become worse. The simulation results show that with an appropriate stepped reflector, better radiation patterns in a wide bandwidth can be generated.

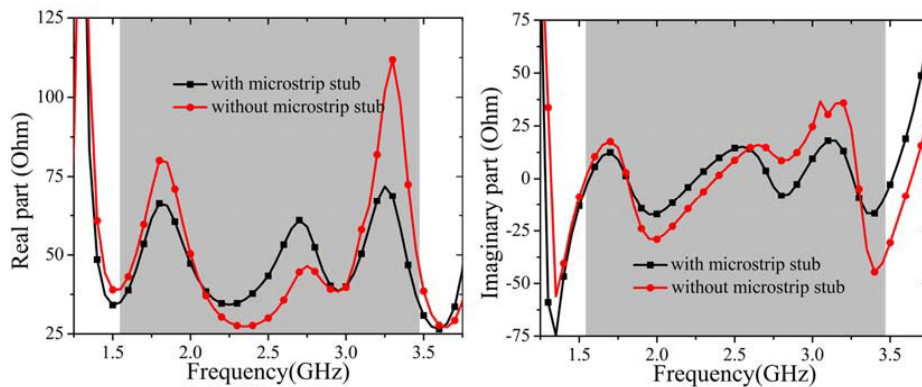


**Figure 2.** Comparison of the input impedance between the antennas with and without the microstrip stub.

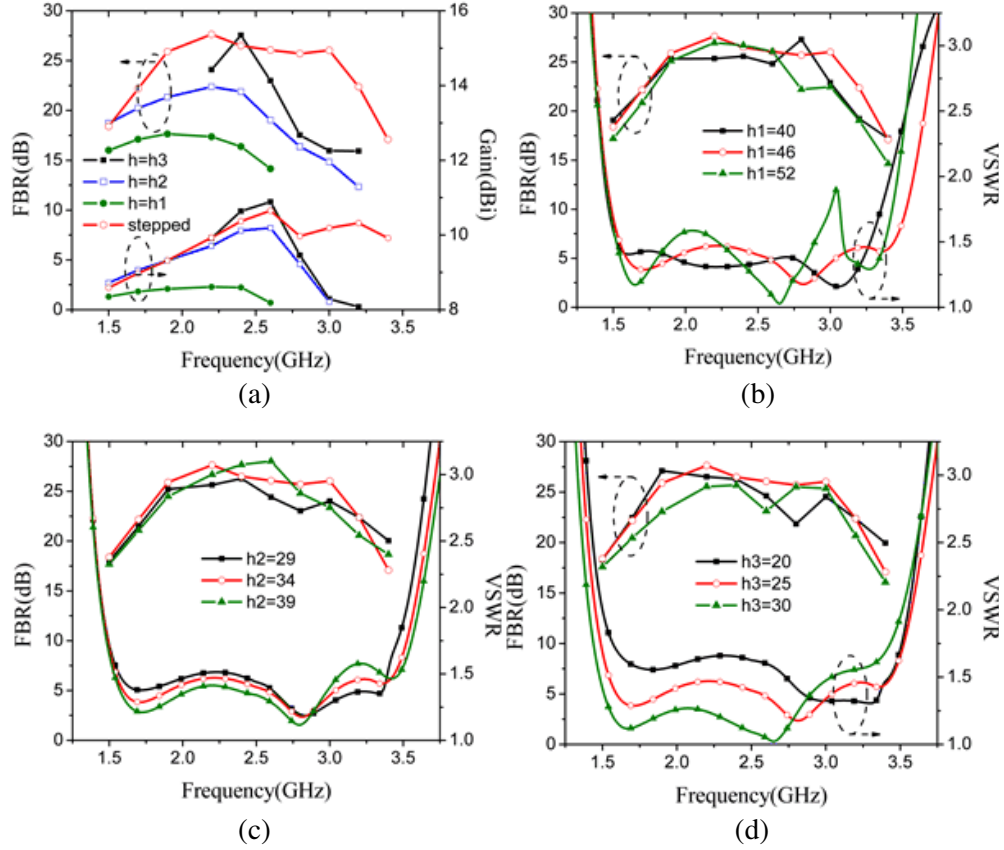


**Figure 3.** (a) Gains and FBRs for antennas with stepped reflector and with single-plate reflector, (b) FBRs and VSWRs for different values of  $h_1$ , (c) FBRs and VSWRs for different values of  $h_2$ , and (d) FBRs and VSWRs for different values of  $h_3$ . (Units: mm).

To evaluate the effects of the reflector's dimensions on the FBRs and VSWRs, a parametric study is performed. The simulated FBRs and VSWRs for the proposed antenna with varying  $h_1$ ,  $h_2$  and  $h_3$  are shown in Figs. 3(b), 3(c) and 3(d), respectively. Fig. 3(b) demonstrates that parameter  $h_1$  affects all the resonance frequencies of the proposed antenna. That is because  $h_1$  is the distance between the driven antennas feeding point and the reflector. When  $h_1$  varies, the currents on the driven antenna change, and then the resonance frequencies shift. From Fig. 3(c), it can be seen that the middle and highest resonance frequencies change when  $h_2$  increases.  $h_2$  is calculated as the quarter wavelength of the middle resonance frequency. When  $h_2$  varies, the currents on the microstrip stubs change. From Fig. 2, it is indicated that the microstrip stubs have great influence on the middle and highest resonance frequencies. Thus,  $h_2$  influences middle and highest resonance frequencies greatly. Fig. 3(d) shows the variation of VSWRs and FBRs with the increase of the parameter  $h_3$ . With increasing  $h_3$ , the lowest frequency expands to lower resonant frequency band.  $h_3$  mainly influences the current on the edges of the disc slots and then has an effect on the lowest resonance frequency. In order to get a better

**Table 1.** Dimension of the proposed antenna. (Units: mm).

Parameters	$W_1$	$W_2$	$W_3$	$W_4$	$W_5$	$W_6$	$W_7$	$W_8$	$L$	$L_1$	$L_2$	$L_3$	$L_4$	$L_5$	$L_6$
values	50	27	11	28	1.7	2.4	1.4	17	120	20	11	17.5	26	2.8	24
parameters	$L_7$	$L_8$	$L_9$	$L_{10}$	$L_{11}$	$L_{12}$	$R$	$R_1$	$R_2$	$h$	$h_1$	$h_2$	$h_3$	$g$	$L_m$
values	16	20	7	22	5	10	8	6	3	10	46	34	25	3.3	7.6

performance, based on the analysis above,  $h_1$ ,  $h_2$  and  $h_3$  are selected as 46 mm, 34 mm and 25 mm, respectively. Other parameters are optimized and adjusted by using ANSYS HFSS. The final parameters used in this design are shown in Table 1.

### 3. RESULTS AND DISCUSSION

The wideband unidirectional slot antenna was simulated by the ANSYS high-frequency structure simulator. Photographs of the proposed unidirectional slot antenna are shown in Fig. 4. The antenna was simulated, manufactured and measured.  $S$ -parameters are measured by using Agilent E5062A Network Analyzer, and the radiation patterns are measured in Tri-L Solutions' Dart 3300 microwave anechoic chamber.

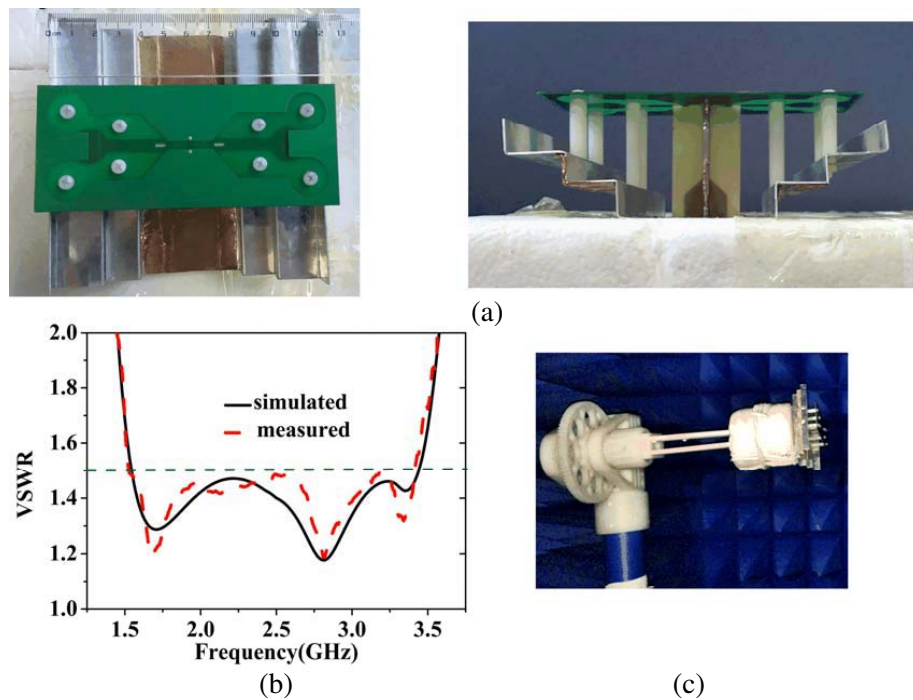


**Figure 4.** (a) Photographs of the fabricated prototype, (b) simulated and measured VSWRs for the proposed antenna, and (c) measurement environment for radiation patterns.

#### 3.1. VSWR

The antenna was fabricated as shown in Fig. 4. The simulated results show that the antenna has an impedance bandwidth of 76% (1.55–3.44 GHz) for  $VSWR \leq 1.5$ , and the measured results indicate that the antenna obtains an impedance bandwidth of 76% (1.53–3.41 GHz), which agrees well with the simulated one.

#### 3.2. Radiation Patterns

The simulated and measured radiation patterns of the proposed antenna at 1.6 GHz, 2.2 GHz, 2.8 GHz and 3.3 GHz are shown in Fig. 5. As shown in the figure, the simulated and measured results are in good agreement. Unidirectional radiation patterns for both the simulated and measured results are obtained. The backward radiations are suppressed due to the stepped reflector. In addition, it is observed that the cross-polarizations in the main radiation directions at 1.6 GHz, 2.2 GHz, 2.8 GHz and 3.3 GHz are less than  $-26$  dB, respectively.

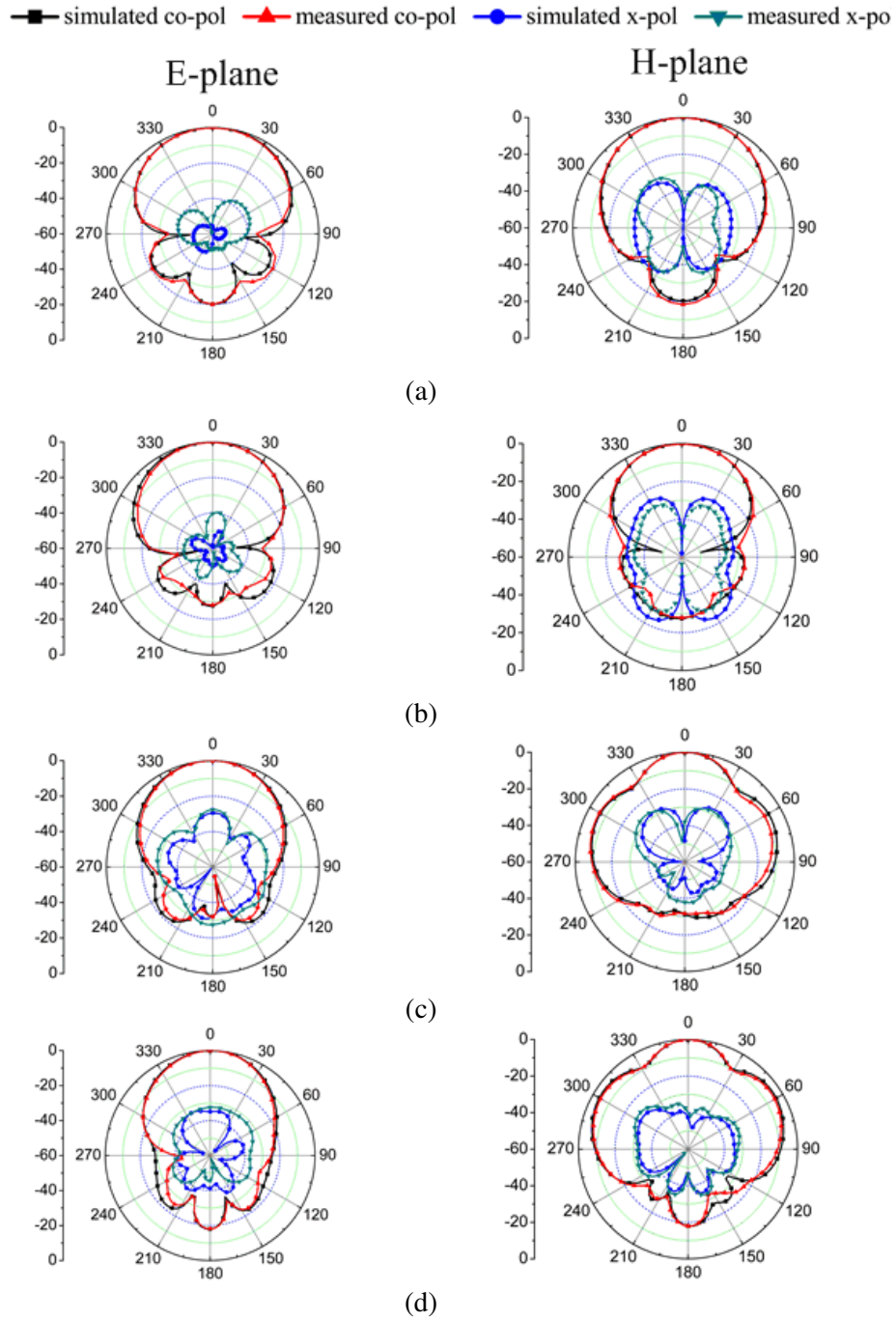


**Figure 5.** Measured and simulated radiation patterns for the proposed antenna. (a) 1.6 GHz, (b) 2.2 GHz, (c) 2.8 GHz and (d) 3.3 GHz.

The simulated and measured gains and FBRs of the proposed antenna are shown in Fig. 6. As shown in the figure, the proposed antenna has a peak gain and peak FBR of 10.4 dBi and 28.6 dB. Within the operating band 1.53–3.41 GHz, the measured and simulated results show that the antenna has gains higher than 8.6 dBi and FBRs greater than 20 dB, except 19 dB at 3.3 GHz and 18 dB at 3.4 GHz due to the distortion of the radiation pattern at high frequency band. Fig. 6 demonstrates that a good agreement can be seen between the simulated and measured gain results.

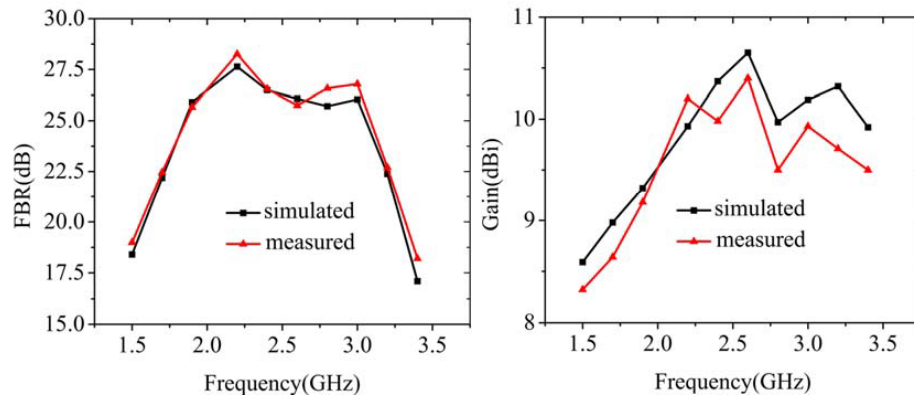


**Figure 6.** Simulated and measured gains and FBRs for the proposed antenna.

The measured results have little deviation from the simulated ones, and the two results match reasonably with each other. Differences between the simulated and measured results are mainly caused by tolerances in the manufacturing process and measurements, such as feed probe mismatch, permittivity inaccuracy, fabrication imperfections and measurement circumstance.

### 3.3. Comparisons

Comparisons between the proposed antenna and some related antennas in dimensions, impedance bandwidth, gain bandwidth and FBR bandwidth have been shown in Table 2. Those antennas have nearly the same frequency range and are used for wireless communications. As shown in the table, the proposed antenna possesses higher gains and greater FBRs than the folded bow-tie antenna in [7]. Moreover, the dimensions of this antenna are much smaller than the antenna in [7]. The proposed antenna has nearly the same dimensions but simultaneously possesses higher gains and greater FBRs than the antenna in [8]. The gain bandwidth and peak gain also increase. Meanwhile, both of the antennas aim for high FBRs, and the FBR bandwidth as well as peak FBR also improves for the proposed antenna. Calculation of dimensions for antenna in [9] does not include the large ground plane. The antenna in [9] is a multilayered Yagi antenna and possesses large dimensions to get high gains and

**Table 2.** Comparisons between the proposed antenna and some related antennas.

antenna	Dimensions (mm <sup>3</sup> )	Impedance bandwidth	Gain Bandwidth (dBi)	FBR Bandwidth (dB)	Max gain/FBR (dBi/dB)
[7]	180 * 105 * 34	1.58–2.89 GHz (58.6% VSWR ≤ 1.5)	1.58–2.89 GHz (58.6% Gains ≥ 8)	1.58–2.89 GHz (58.6% FBRs ≥ 17)	9.4/-
[8]	120 * 120 * 40	1.66–2.83 GHz (52.1% VSWR ≤ 1.5)	1.66–2.83 GHz (52.1% Gains ≥ 7.1)	1.66–2.83 GHz (52.1% FBRs ≥ 18.6)	7.8/25
[9]	> 90 * 56 * 130	1.34–2.83 GHz (70.8% VSWR ≤ 2)	1.34–2.83 GHz (70.8% Gains ≥ 10.8)	1.34–2.83 GHz (70.8% FBRs ≥ 20)	12.5/28
[10]	150 * 120 * 55	1.2–2.76 GHz (77% VSWR ≤ 2)	≈ 1.3–2.6 GHz (66% Gains ≥ 8.5)	≈ 1.4–2.8 GHz (66% FBRs ≥ 12)	10.1/16.7
[11]	150 * 120 * 40	1.37–3.21 GHz (80.35% VSWR ≤ 2)	1.56–3.14 GHz (67% Gains ≥ 8.5)	1.56–3.14 GHz (67% FBRs ≥ 17)	≈ 9/22
proposed	120 * 120 * 46	1.53–3.41 GHz (76% VSWR ≤ 1.5)	1.53–3.41 GHz (76% Gains ≥ 8.6)	1.53–3.41 GHz (76% FBRs ≥ 18.2)	10.4/28.6

good FBRs. It can be seen that the proposed slot antenna has a nearly same impedance bandwidth but simultaneously possesses higher gains and greater FBRs than the adjustable back-reflector antenna in [10]. The gain bandwidth has an increase about 16%. Meanwhile, the FBR bandwidth has been improved greatly. Comparisons between the proposed antenna and the microstrip-fed antenna in [11] indicate that a size reduction about 8% has been achieved. However, the gain bandwidth (gains higher than 8.5 dBi) has an increase about 15%. Considering the significant improvement that has been obtained in impedance bandwidth, antenna gains and FBRs, the proposed antenna can be widely used in wireless communication.

#### 4. CONCLUSIONS

In this paper, a compact unidirectional wideband slot antenna is proposed. The antenna consists of a novel compact slot driven antenna, a stepped reflector and a vertical balun. With the balun and microstrip stubs, the antenna can get an impedance bandwidth of 76% (1.53–3.41 GHz) for the  $VSWR \leq 1.5$ . And by optimizing the height of the stepped reflector, the antenna can obtain gains higher than 8.6 dBi, FBRs around 22 dB, and a cross-polarization less than  $-26$  dB. All these properties indicate that the proposed antenna is a good candidate for wireless application.

#### ACKNOWLEDGMENT

This work was supported in part by the National Natural Science Foundation of China under Grant No. 61201022, and in part by the Fundamental Research Funds for the Central Universities under Grant No. JB150224.

#### REFERENCES

1. Nakano, H. and J. Yamauchi, "Printed slot and wire antenna: A review," *Proceedings of the IEEE*, Vol. 100, No. 7, 2158–2168, Jul. 2012.
2. Yun, S., D.-Y. Kim, and S. Nam, "Bandwidth enhancement of cavity-backed slot antenna using a via-hole above the slot," *IEEE Antennas Wireless Propag. Lett.*, Vol. 11, 1092–1095, 2012.
3. Chair, R., A. A. Kishk, K. F. Lee, and C. E. Smith, "Unidirectional wideband slot aperture antennas," *IEEE Antennas and Propagation Society International Symposium (APSURSI)*, 1875–1878, 2004.
4. Wang, C. J. and Y. Dai, "Enhancement of pattern directivity for the open slot antenna by utilizing array topology," *Microwave Opt. Technol. Lett.*, Vol. 54, No. 5, 1273–1277, Mar. 2012.
5. Chen, W. Q., G. F. Ding, B. H. Li, and X. F. Li, "Design and simulation of broadband unidirectional CPW-fed rectangular slot antennas," *IEEE International Conference on Microwave, Antennas, Propagation and EMC Technologies for Wireless Communications (MAPE)*, 632–635, 2007.
6. Chaimool, S., P. Akkaraekthalin, and M. Krairiksh, "Reflector shape optimization for wideband uni-directional of CPW-fed slot antenna," *International Symposium on Antennas and Propagation, (ISAP)*, 1206–1209, 2007.
7. Zhang, Z. Y., S.-L. Zuo, and J. Y. Zhao, "Wideband folded bowtie antenna with  $\Gamma$ -shaped strip feed and tuning stubs," *Microwave Opt. Technol. Lett.*, Vol. 55, No. 9, 2145–2149, Jun. 2013.
8. Govindanarayanan, I. and N. Rangaswamy, "Asymmetric folded dipole antenna with high front to back ratio for LTE base stations," *IEEE Antennas Wireless Propag. Lett.*, Vol. 15, 869–872, 2016.
9. Wang, Z. D., X. L. Liu, Y. Z. Yin, and J. J. Wu, "Dual-element folded dipole design for broadband multilayered Yagi antenna for 2G/3G/LTE applications," *Electron Lett.*, Vol. 50, No. 4, 242–244, Feb. 2014.
10. Fei, P., Y. H. Qi, and Y. C. Jiao, "Design of a wideband dual-element slot loop antenna array with adjustable back-reflector," *IEEE Antennas Wireless Propag. Lett.*, Vol. 11, 1014–1017, 2012.
11. Gao, X. Y., Y. H. Qi, and Y. C. Jiao, "Design of multiplate back-reflector for a wideband slot antenna," *IEEE Antennas Wireless Propag. Lett.*, Vol. 12, 773–776, 2013.